Laboratori Nazionali di Frascati

LNF-61/37 (9.7.61)

G. Da Prato: SINGLE PION PRODUCTION IN PROTON PROTON COLLISIONS ACCORDING TO THE ONE PARTICLE EXCHANGE MODEL.

Laboratori Nazionali di Frascati del C.N.E.N.
Servizio Documentazione

Nota interna n° 85
9 Luglio 1961.

G. Da Prato: SINGLE PION PRODUCTION IN PROTON-PROTON COLLISIONS ACCORDING TO THE ONE-PARTICLE EXCHANGE MODEL.-

Abstract

Single pion production in nucleon-nucleon collisions is calculated in the one pion exchang approximation. All the possible diagrams of this kind are calculated in the "pole" approximation discussed in the text; also the interferences between them are taken into account.

The lab. energy spectra of the final nucleons are calculated and compared with the experimental data at 2.85 GeV.

This comparison shows a remarkably good agreement for small values of the squared 4-momentum of the virtual pion.

For higher values the qualitative behaviour is still reproduced, but the theoretical absolute values are larger than the experimental ones.

I. Introduction

We want to study the processes of single pion production in proton-proton collisions, namely the reactions:

$$p+p = p+n+\pi^{+} \qquad (1)$$

$$p+p = p+p+\pi^{0} \qquad (2)$$

by using the model which describes the processes as occurring through the exchange of a single pion (Fig. 1).

This approach has been suggested by the fact that, in the last years, experimental evidence has been produced that in high energy inelastic processes small momentum transfer of the recoiling target particle are strongly favoured [1].

This situation can be qualitatively explained through a mechanism of interaction due to the exchange of a single pion [2], and for some particular reactions detailed calculations have been performed [3]. The situation, however, is not yet completely clear, because in the quoted papers [3] drastic simplifications have been made, e.g. by neglecting some of the possible one-pion exchange (OPE) diagrams and the various mutual interference terms. New detailed experimental data on single pion production in proton-proton collision have recently been obtained at 2.85 GeV of the incident proton in the lab. system [4].

In the laboratory energy spectra of the final nucleons one finds again strong peaks corresponding to very small momentum transfers. This indicates again that the one-particle exchange plays an important role in the particular processes (1) and (2). We think it useful to calculate the spectra predicted by this model in the whole physical region by taking into account all the

possible OPE effects. By comparing the prediction of the model with the experiment, we expect to find a sensibly good agreement in the region of small momentum transfers, where the further approximations made in order to obtain quantitative numerical results [5] can be well justified. These approximations consist in neglecting the influence of the "pion form factors" of the upper vertex in Fig. 1 and of the propagator of the virtual pion; and in considering as Δ^2-independent [6] the partial wave amplitudes for the "off shell" pion-nucleon scattering. (The scattering angle which enters in the description of the lower vertex [5] is not taken on shell, but its dependence on Δ^2 is taken into account). For the region of higher momentum transfers we know a priori that these approximations are not good, but the comparison of the theory with the experiment can always give us a suggestion for approaching the problem of the OPE contribution when the intermediate particle is very virtual. We expect in this region to obtain an overestimate of the OPE contribution, which in all probability is mainly due to the neglected effects of the "pionic form factor" in the upper vertex of Fig. 1. Also the calculation of the interference effects generally involves at least one of the interfering terms considerably off shell. In this paper, however, it will be seen that these effects are not so important, and, in some cases, they turn out to be negligible.

Section 2 will be dedicated to notations and kinematics, Section 3 to the study of the lower vertex, Section 4 to the calculation of the differential cross-sections and finally Section 5 to the discussion of the obtained results.

II. Notations, kinematics, Feynman graphs

We denote by p_1, k_1, p_2, k_2, q_2 the energy-momentum 4-vectors of the incoming proton, target proton, outgoing proton, outgoing neutron (proton) for the first (second) reaction and outgoing pion respectively. We indicate by μ the pion mass and M the nucleon mass. Forthermore, we define the kinematical invariants

$$w^2 = -(p_1+k_1)^2, l^2 = -(k_2+q_2)^2, u^2 = -(p_2+q_2)^2, \Delta^2 = (k_2-k_1)^2, r^2 = \tag{3}$$

$$= (k_2-p_1)^2, s^2 = (p_2-k_1)^2, t^2 = (p_2-p_1)^2$$

Among them the following relations hold

$$\Delta^2+r^2+u^2 = s^2+t^2+l^2 = w^2-3M^2 \tag{4}$$

w, l, u, are respectively: the total c.m. energy, the energy of k_2 and q_2 in their c.m. system and the energy of p_2 and q_2 in their c.m. system. Δ^2, r^2, s^2, t^2 are nucleon momentum transfer.
Five of the invariants (3) are sufficient to obtain a complete description of the kinematics.

We will use also the following quantities:

a) In the c.m. system of p_2 and q_2 χ' is the 3-momentum of p_2 and q_2, p'_{10}, k'_{10}, p'_{20}, k'_{20}, q'_{20} are the energies of p_1, k_1, p_2, k_2, q_2 respectively, ε' is the angle between p_2 and p_1, β' the angle between p_2 and k_1, α' the angle between p_1 and k_1, φ' is the p_2 azimuthal angle in a frame of reference with the z axis directed along p_1.

b) In the c.m. system of p_2 and k_2 the same quantities will be denoted by $\varkappa''$, p''_{10}, k''_{10}, p''_{20}, k''_{20}, q''_{20}, ε'', β'', α'', φ'', respectively. Finally $T_L(p_2)$ and $T_L(k_2)$ will be the lab. kinetic energies of particles p_2 and k_2 respectively and k the 3-momentum of p_1 and k_1 in the c.m. system. We have)

$$T_L(k_2) = \frac{\Delta^2}{2M} \qquad T_L(p_2') = \frac{s^2}{2M} \tag{5}$$

The expression of the other kinematical quantities as functions of the invariants are given in [5].

The T matrix is defined by

$$S_{fi} = \delta_{fi} + \frac{iM^2 \delta^4(p_2+k_2+q_2-p_1-k_1)}{2(2\pi)^{7/2}(p_{10}k_{10}p_{20}k_{20}q_{20})^{1/2}} T_{fi} \tag{6}$$

p_{10}, k_{10}, p_{20}, k_{20}, q_{20} are the energies in an arbitrary frame of reference. The differential cross-section $d\sigma$ is given by

$$d\sigma = \frac{M^4}{2(2\pi)^5 KW} \overline{\sum_{spin}} |T_{fi}|^2 \delta^4(p_2+k_2+q_2-p_1-k_1) \frac{d^3p_2 d^3k_2 d^3q_2}{p_{20}k_{20}q_{20}} \tag{7}$$

The bar over the summation index indicates the average over initial spins. Formula (7) is equivalent to:

$$d\sigma = \frac{M^4}{8(2\pi)^4 K^2 W^2} \overline{\sum_{spin}} |T_{fi}|^2 \frac{\varkappa'}{\omega} d\cos\varepsilon' d\varphi' du^2 d\Delta^2 \tag{8}$$

and also equivalent to

$$d\sigma = \frac{M^4}{8(2\pi)^4 K^2 W^2} \overline{\sum_{spin}} |T_{fi}|^2 \frac{\varkappa''}{\omega} d\cos\varepsilon'' d\varphi'' dl^2 ds^2 \tag{9}$$

We shall use (8) for the k_2 particle spectrum and (9) for the p_2 particle spectrum.

The allowed physical region is determined from the following relations

$$0 \leq \varphi' \leq 2\pi \tag{10}$$

$$0 \leq \varepsilon' \leq \pi \tag{11}$$

$$(M+\mu)^2 \leq u^2 \leq \left\{ M^2+W^2/2M^2 \left[2K(\Delta^4+4M^2\Delta^2)^{\frac{1}{2}} - \Delta^2 W \right] \right\} \tag{12}$$

$$\begin{aligned} &\tfrac{1}{2}\left\{W^2-\mu^2-2M\mu-4M^2-K/W\left[(W^2-\mu^2-2M\mu)^2-4M^2W^2\right]^{\frac{1}{2}}\right\} \leq \Delta^2 \leq \tfrac{1}{2} \\ &\left\{W^2-\mu^2-2M\mu-4M^2+K/W\cdot\left[(W^2-\mu^2-2M\mu)^2-4M^2W^2\right]^{\frac{1}{2}}\right\} \end{aligned} \tag{13}$$

for the case (8), and by the relations which we obtain by exchanging $\varphi' \to \varphi''$, $\varepsilon' \to \varepsilon''$, $u^2 \to l^2$, $\Delta^2 \to s^2$ for the case (9).

The four possible Feynman graphs are given in Fig. 2.

Let T_i^u and T_i^l be the T matrix elements relative to upper and lower vertices of i^{th} graph. We have

$$T_{fi} = \left[\frac{\langle T_1^u \rangle \langle T_1^l \rangle}{\Delta^2+\mu^2} + \frac{\langle T_3^u \rangle \langle T_3^l \rangle}{s^2+\mu^2} - \frac{\langle T_2^u \rangle \langle T_2^l \rangle}{r^2+\mu^2} - \frac{\langle T_4^u \rangle \langle T_4^l \rangle}{t^2+\mu^2} \right] \tag{14}$$

for the reaction (1) and

$$T_{fi} = \left[\frac{\langle T_1^u \rangle \langle T_1^l \rangle}{\Delta^2+\mu^2} + \frac{\langle T_4^u \rangle \langle T_4^l \rangle}{t^2+\mu^2} - \frac{\langle T_2^u \rangle \langle T_2^l \rangle}{r^2+\mu^2} - \frac{\langle T_3^u \rangle \langle T_3^l \rangle}{s^2+\mu^2} \right] \tag{15}$$

for the reaction (2). The minus signs are due to the Pauli principle [7].

III. Pion-nucleon scattering amplitude

Let p_1 and p_2 be the energy-momentum 4-vectors of the nucleons, and q_1 and q_2 those of the pions. We consider first the physical process; then $q_1^2 = -\mu^2$. The T matrix elements are of the following form [8]

$$\langle T^1 \rangle = \bar{u}(p_2)(-A+iBq_2)u(p_1) \tag{16}$$

$u(p_2)$ and $u(p_1)$ are the nucleon spinors and A and B are given by

$$\begin{cases} A = 4\pi \left(f_1 \dfrac{u + M}{p'_{20}+M} - f_2 \dfrac{u - M}{p'_{20}-M} \right) \\ B = 4\pi \left(f_1 \dfrac{1}{p'_{20}+M} + f_2 \dfrac{1}{p'_{20}-M} \right) \end{cases} \tag{17}$$

with

$$\begin{cases} f_1 = \sum_{l=0}^{l=\infty} f_l + p'_{l+1}(\cos \varepsilon') - \sum_{l=2}^{l=\infty} f_l - p'_{l-1}(\cos \varepsilon') \\ f_2 = \sum_{l=1}^{l=\infty} (f_l - f_{lr})\, p'_l\, (\cos \varepsilon') \end{cases} \tag{18}$$

u is the total c.m. energy, p'_{20} is the nucleon energy and ε' the scattering angle in the c.m. system p'_l are derivative of Legendre polinomials. When q_1 goes off shell ($q_1^2 = \Delta^2$) formula (17) is modified in the following way

$$A(u^2,\Delta^2) = 4\pi\left[f_1(u^2,\Delta^2,t^2)\frac{u+M}{\sqrt{(p'_{10}+M)(p'_{20}+M)}} - f_2(u^2,\Delta^2,t^2)\frac{u-M}{\sqrt{(p'_{10}-M)(p'_{20}-M)}}\right]$$

(19)

$$B(u^2,\Delta^2) = 4\pi\left[f_1(u^2,\Delta^2,t^2)\frac{1}{\sqrt{(p'_{10}+M)(p'_{20}+M)}} + f_2(u^2,\Delta^2,t^2)\frac{1}{\sqrt{(p'_{10}-M)(p'_{20}-M)}}\right]$$

This definition leaves unchanged the bidimensional representation of the T matrix elements [8] where the only Δ^2 dependence is contained in f_1 and f_2 **). In the expression (18) the whole t^2 dependence is contained in $\cos\xi'$, which can be easily "extrapolated" off shell by means of its definition

$$\cos\xi' = \frac{2p'_{10}p'_{20} - 2M^2 - t^2}{2|p'_1||p'_2|} \qquad (20)$$

while the amplitude $f_{1\pm}$ are considered as Δ^2-independent. This procedure can be trusted at low Δ^2; but it is at present the simplest one and gives the extension of Chew and Low's formula [9] to the whole physical region.

Quantities (19) will be used in the calculation of graph 1. In graph 2, 3, 4 we have as arguments of A and B u^2r^2, l^2s^2, l^2t^2 respectively [10].

**) See also (5) for a discussion of this subject.

The reactions occurring in the lower vertex are:

$$\pi^+ + p \rightarrow \pi^+ + p \tag{21}$$

$$\pi^0 + p \rightarrow \pi^+ + n \tag{22}$$

for reaction 1 and

$$\pi^0 + p \rightarrow \pi^0 + p \tag{23}$$

for reaction 2.

Reaction (21) is in a pure 3/2 isotopic state and the only important wave is the $p^{3/2}$ wave. For this reason for the calculations of $\langle T^{\ell} \rangle$ relative to (21) we have considered only f_{1+} different from 0; we use for it the one resonance level formula [11]

$$\begin{cases} f_{1+}(u) = \dfrac{1}{2\chi^3} \dfrac{\sqrt{\Gamma_1}}{(u_1 - u) - i\dfrac{\sqrt{\Gamma_1}}{2}} \\ \\ \Gamma_1 = \dfrac{2(\chi a)^3}{1+(\chi a)^2} \gamma_\lambda^2 \end{cases} \tag{24}$$

with $a = 5.91$, $\gamma_\lambda^2 = 0.0625$, $u_1 = 1.314$ in units of proton mass [12].
Reaction (22) contains a mixture of 3/2 and 1/2 isotopic spin states. With increasing energy $p^{3/2}_{3/2}$, $D^{1/2}_{3/2}$, $F^{1/2}_{5/2}$ waves become, in turn, dominant.
In this case we have considered different from 0 only

$$f_{1+}^{3/2} \text{ for } u \leq 1.51 \tag{25}$$

$$f_{2-}^{1/2} \text{ for } u \quad 1.51 \leq u \leq 1.69 \tag{26}$$

$$f_{3-}^{1/2} \text{ for } u \geq 1.69 \tag{27}$$

f_{2-} and f_{3-} have been calculated by empirical formulas from the latest experimental data [13]. We obtain

$$f_{2-}(u) = \frac{1}{2{,}288\,\chi} \frac{\Gamma_2}{(u_2-u)i - \frac{\Gamma_2}{2}} \tag{28}$$

$$\Gamma_2 = 68{,}23u^3 - 315{,}30u^2 + 485{,}21u - 248{,}47$$

$$u_2 = 1.619 \tag{29}$$

$$f_{3-}(u) = \frac{1}{2\chi} \frac{\Gamma_3}{(u_3-u)i\,\frac{\Gamma_3}{2}} \tag{30}$$

$$\Gamma_3 = -7{,}96u^3 + 48{,}33u^2 - 96{,}27u + 63{,}27$$

$$u_3 = 1{,}800 \tag{31}$$

Reaction (23) contains also a mixture of isotopic spin states. $P^{3/2}$ waves are dominant in interval (25), $D^{3/2}$ and $F^{5/2}$ waves in intervals (26) and (27), but in the latter cases the $P^{3/2}$ wave is not negligible with respect to $D^{3/2}$ and $F^{5/2}$ waves, because it enters multiplied to a factor of 4 (when squared). For this reason the calculations relative to reaction (2) are somewhat more complicated than those relative to reaction (1). In the next section we will first consider reaction (1) and on this basis we will obtain a good approximation for the calculations of reaction (2).

VI. Spin summation

By substituting in (14) the $\langle T_i^u \rangle$ calculated with the usual Feynman rules and the $\langle T_i^\ell \rangle$ obtained from (16) and (20), and finally by averaging over initial and summing over final spins we obtain for the first reaction

$$T_{fi} = F_1(u^2, \ell^2, \Delta^2, s^2) + F_1(u^2, \ell^2, r^2, t^2) + 1/9 F_1(\ell^2, u^2, s^2, \Delta^2) +$$

$$+ 1/9 F_1(\ell^2, u^2, t^2, r^2) + 1/3 F_2(u^2, \ell^2, \Delta^2, s^2) + 1/3 F_2(\ell^2, u^2, s^2, \Delta^2) + \qquad (32)$$

$$+ 1/3 F_3(u^2, \ell^2, \Delta^2, s^2) + 1/3 F_3(u^2, \ell^2, r^2, t^2)$$

with

$$F_1(u^2, \ell^2, \Delta^2, s^2) = \frac{2 g^2 u^2 (2\pi)^2}{M^4} \frac{\Delta^2}{(\Delta^2 + \mu^2)^2} R \left[f_1 f_1^* + f_1 f_2^* \cos\xi' + f_2 f_1^* \cos\xi' + f_2 f_2^* \right]$$

$$F_2(u^2, \ell^2, \Delta^2, s^2) = \frac{2(2\pi)^2 g^2}{M^4} \frac{u^2}{(\Delta^2 + \mu^2)(r^2 + \mu^2)} R \left\{ \left[(p'_{10} - M)(k'_{10} - M) \right]^{1/2} \right. \qquad (33)$$

$$\left[f_1 f_1^* \cos\alpha' + f_2 f_2^* + f_1 f_2^* \cos\xi' + f_2 f_1^* \cos\beta'\right] (u+M) + \left[(p'_{10}+M)(k'_{10}+M)\right] 1/2$$

$$\left[f_2 f_2^* \cos\alpha' + f_1 f_1^* + f_2 f_1^* \cos\xi' + f_1 f_2^* \cos\beta'\right] (u-M) \Big\} \qquad (34)$$

$$F_3(u^2, \ell^2, \Delta^2, s^2) = -\frac{g^2}{4M^4} \frac{1}{(\Delta^2+\mu^2)(s^2+\mu^2)} R \Big\{ L\left[AA^* - \mu^2 BB^*\right] -$$

$$-N\left[MBA^* + MAB^* + 2BB^*\right](\chi' |\underline{p}'_1| \cos\xi' + p'_{10}q'_{20}) + P\left[BA^* - AB^*\right] + \quad . \qquad (35)$$

$$+Q\left[2BA^*(\chi' |\underline{p}'_1| \cos\xi' + p'_{10}q'_{10}) + MAA^* + \mu^2 BB^*\right] \Big\}$$

Here the f_i are functions of u^2 and Δ^2; f_i^* are functions of u^2 and Δ^2 in (33), of u^2 and r^2 in (34), of ℓ^2 and s^2 in (35).

We have

$$L = up'_{20}(|\underline{p}'_1||\underline{k}'_1| \cos\alpha' + p'_{10}k'_{10}) - u\chi' k'_{10} |\underline{p}'_1| \cos\xi' - \chi' |\underline{k}'_1| \cos\beta' \qquad (36)$$

$$(up'_{10} - M^2) + M^2(M^2 - up'_{10} - k'_{10}p'_{20})$$

$$N = \chi' |\underline{p}'_1| (uk'_{10} - M^2) + \chi' |\underline{k}'_1| \cos\beta' u(u - p'_{10}) + M^2(\mu^2 - p'_{10}q'_{20}) + \qquad (37)$$

$$+ 1/2(\Delta^2 + 2M^2)(\chi'^2 + p'_{20}q'_{20})$$

$$P = M\left\{\chi' \left|\underline{p}'_{-1}\right| \cos\xi' \left[\underline{W}^2 - 3M^2 + \mu^2 + uk'_{10} + 2p'_{10}(q'_{20} - p'_{20} - k'_{10})\right] + \right.$$

$$+\chi' \left|\underline{k}'_{-1}\right| \cos\beta'(up'_{10} - M^2) + \left|k'_1\right| \left|p'_1\right| \cos\alpha'(2k'_{10} - u) - q'_{20}p'_{10}k'_{10}(k'_{20} - p'_{10} + k'_{10}) +$$

$$\left. + M^2 q'_{20}(p'_{10} - k'_{10}) + p'_{10}q'_{20}(\mu^2 - p'_{10}p'_{20}) + M^2(\chi'^2 + p'_{20}q'_{20})\right\} \qquad (38)$$

$$Q = M\left\{\left|\underline{k}'_{-1}\right| \left|\underline{p}'_{-1}\right| \cos\alpha' - \chi' \left|p'_1\right| \cos\xi' + k'_{10}(u - p'_{10}) + p'_{20}(k'_{20} - k'_{10})\right\} \qquad (39)$$

g^2 is the renormalized pion-nucleon coupling constant

$$g^2 = \frac{4\pi M^2 8^2}{\mu^2} \qquad (40)$$

$$f^2 = 0.08 \qquad (41)$$

The f_1 terms came from square moduli of the single graphs, the F_2 terms from interferences between graphs which differ for the exchange of both initial nucleons, and the F_3 terms from interferences between graphs which differ for the exchange of the final nucleons. The interference terms between graphs which differ for the exchange of both initial and final nucleons vanish. The factor 1/3 and 1/9 are due to isotopic spin.

By putting (32) into (8) and (9) we get the spectra of outgoing nucleons. In case (8) the integrals of the first, the second and the fourth term can be easily reduced to single integrals because the integrands are φ'-independent [5]. We can get a similar reduction also in case (9).

The main contributions to the cross-section are due to the F_1 terms. The F_2 terms give a contribution about five times smaller, the F_3 terms give a negligible contribution. We note also that the F_2 terms are the smaller the larger is the number of waves occurring.

Consider reaction (2). In this case we neglect the interference terms F_3, because they are the same as in the previous case, apart from isotopic spin factors. For the other terms we use formula (33) (without the F_3 terms) with the following additional modifications:

a) A factor 1/18 in front of all the F_1 and F_2 terms

b) For F_1 terms f_1 and f_2 are the same in the interval (25); in the intervals (26) and (27) they assume the following expressions

$$\begin{cases} f_1 = 6f_{1+}\cos\xi' - f_{2-} \\ f_2 = -2f_{1+} + 3f_{2-}\cos\xi' \end{cases} \tag{42}$$

and

$$\begin{cases} f_1 = 6f_{1+}\cos\xi' - 3f_3\cos\xi' \\ f_2 = 2f_{1+} + f_3 - \frac{3}{2}(5\cos^2\xi' - 1) \end{cases} \tag{43}$$

respectively.

V. Concluding remarks

Numerical results at 2.85 GeV for reactions (1) and (2) are shown and compared with experimental data in Figs. 3, 4 and 5. The agreement is very good when the squared four-momentum of the virtual pion is small (of the order of few times the squared π-meson mass). Not only the presence and the exact position of the low and high energy peaks are correctly predicted, but also their absolute normalization is reproduced within the experimental errors. This, to our opinion, definitely suggests that the one-pion exchange contribution plays an important role in the description of processes (1) and (2). Let us analyse the general behaviour of figures 3 and 4 referring to reaction (1).

As we said already in the text, all the interferences between the diagrams in Fig. 2 turn out to be small. Therefore, we can discuss, in a first approximation, the four diagrams separately. The largest contribution is always given from the graphs 1 and 2 of Fig. 2. Where the π^+ comes out with the proton and allows the formation of the pure T=J=3/2 resonance. The squared matrix element of graph 1 contains the factor $\Delta^2(\Delta^2+\mu^2)^{-2}$ which would give alone a steep maximum at $\Delta^2 \simeq \mu^2$. The further Δ^2 dependence of the cross-section, given from the phase space limitations on the integration over the other dynamical variables, shifts this maximum to $\Delta^2 \simeq 2\mu^2$. Due to the proportionality of Δ^2 to the lab. neutron energy, this gives the low energy peak in Fig. 3. The high energy peak, which exists again for low values of the squared four-momentum of the virtual pion (r^2 this time), is contributed from graph 2. Its existence can be understood as follows. Graph 1 gives a strong backward peak of the neutrons in the c.m. angular distribution. Graph 2 gives a symmetric c.m. forward peak. The fact that these diagrams give a symmetric contribution is simply an effect of the Pauli principle, stating that all the final particles in a reaction in which the initial ones are identical, must have a c.m. angular distribution symmetric around 90°. The forward neutrons

in c.m. will then give rise to the high energy peak in the lab. system, while the backward ones give rise to the low energy peak. This effect is enhanced to the presence of the 33 resonance in the lower vertices. For the proton spectrum the argument is similar, though a little more complicated. The protons from graphs 1 and 2 are coming out together with a π^+. Tendency of formation of the 33 isobar will be shown. It should be clear that since the c.m. angular distribution of the "isobar" is the same as that of the neutron and since the proton is much heavier than the pion (the kinetic relative energy being small), its angular distribution will again be peaked forward and backward, though less markedly than for the neutron. Therefore, again, we should expect high and low energy peaks in the proton lab. spectra, of course broader than in the neutron case. Practically the high energy peak the broadening is so large that the peak disappears, but in any case we have a concentration of events at high energy.

Similar considerations hold also for reaction (2): in this case, further complications arise from the fact that all the 4 diagrams have the same weight and that in all of them d and f waves are present. The qualitative features discussed above can be, however, easily extended also to this case.

VI. Acknowledgements

We thank Professor L. Van Hove for kind hospitality in the theoretical group at CERN, where an important part of this work has been carried out. We thank also the CERN Ferranti computer staff for invaluable help in the numerical calculations. We thank Drs. E. Ferrari and F. Selleri for very useful suggestions and for continuous advice. We are indebted also to Professor R. Gatto for his interest in this work.

REFERENCES

1) J.G. Rushbrooke and D. Radojicic, Phys. Rev. Letters 5, 567 (1950)
A.P. Batson et. al., Proc. Roy. Soc. (London) 251, 218 (1959)

2) See for instance: F. Salzman and G. Salzman, Phys. Rev. 120, 599 (1960)

3) E. Ferrari, Nuovo Cimento 15, 652 (1960) and Phys. Rev. 120, 988 (1960)
S.D. Drell, Phys. Rev. Letters 5, 278 (1960) and
Phys. Rev. Letters 5, 342 (1960)
F. Salzman and G. Salzman, Phys. Rev. Letters 5, 377 (1960)
J. Iizuka and A. Klein, University of Pennsylvania, preprint
F. Selleri, Phys. Rev. Letters 6, 64 (1961)
In the last two papers an error of normalization is contained. In both cases the theoretical predictions would be correct if multiplied by two

4) G.A. Smith, H. Courant, E.C. Fowler, H. Kraybill, J. Sandweiss and H. Taft, Yale University, preprint
The experimental lab. energy spectra used in this paper are a private communication of the above authors
We thank Dr. G.A. Smith and Prof. H. Taft for having sent us these data.

5) E. Ferrari and F. Selleri, to be published

6) Here we denote by Δ^2 the square of the 4-momentum of the intermediate particle. We use the metric $p^2 = |\mathbf{p}|^2 - p_o^2$

7) Brackets stand for indices fi.

8) G.F. Chew, M.L. Goldberger, F.E. Low, Y. Nambu, Phys. Rev. 106, 1337 (1957)

9) G.F. Chew and F.E. Low, Phys. Rev. 113, 1640 (1959)

10) In the following, we shall write $A(u^2, \Delta^2)$ instead of (u^2, Δ^2, t^2) and so on: the obvious momentum transfer dependence is dropped for simplicity

11) M. Gell-Mann and K. Watson, Annual Review of Nuclear Science (Annual Reviews Inc., Palo Alto, California, 1954) Vol. 4, p. 219

12) We will express in the following all numerical results in units of proton mass, unless otherwise stated.

13) P. Falk-Vairant and G. Valladas, Centre d'Etudes Nucléaires de Saclay, rapport à la conférence de Rochester 1960

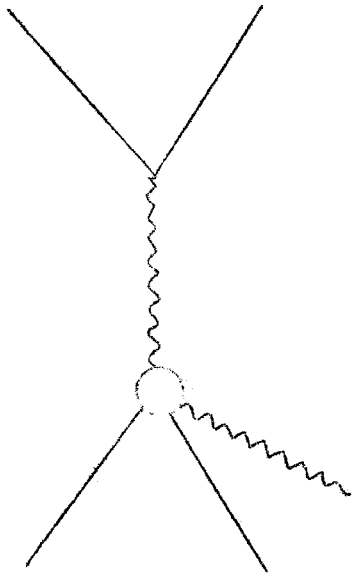

Fig. 1 OPE diagram for the description of process (1) or (2). Full lines represent nucleons, dashed lines represent pions.

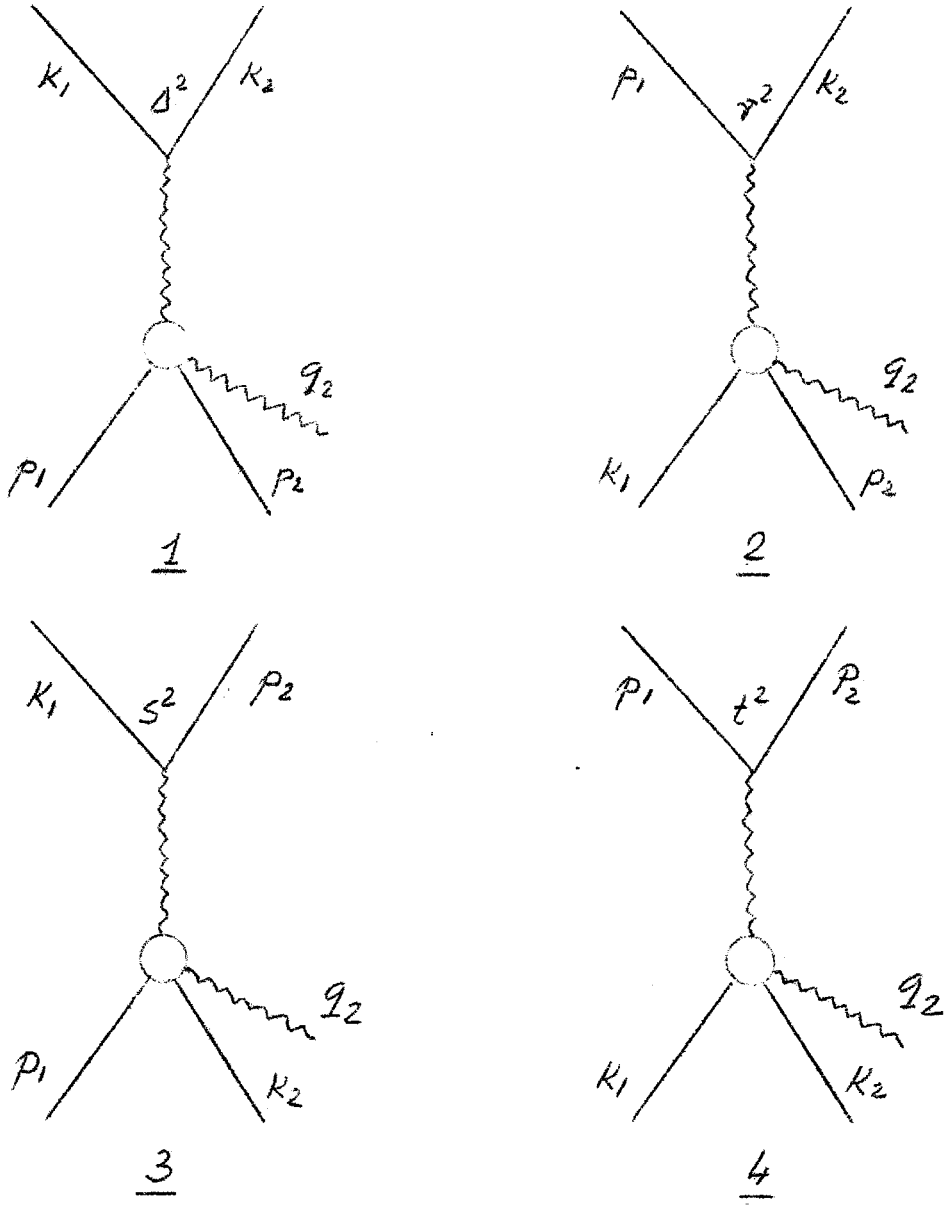

Fig. 2 The possible OPE Feyman graphs for the process (1) or (2). In the upper certiccs are written the relative momentum transfer.

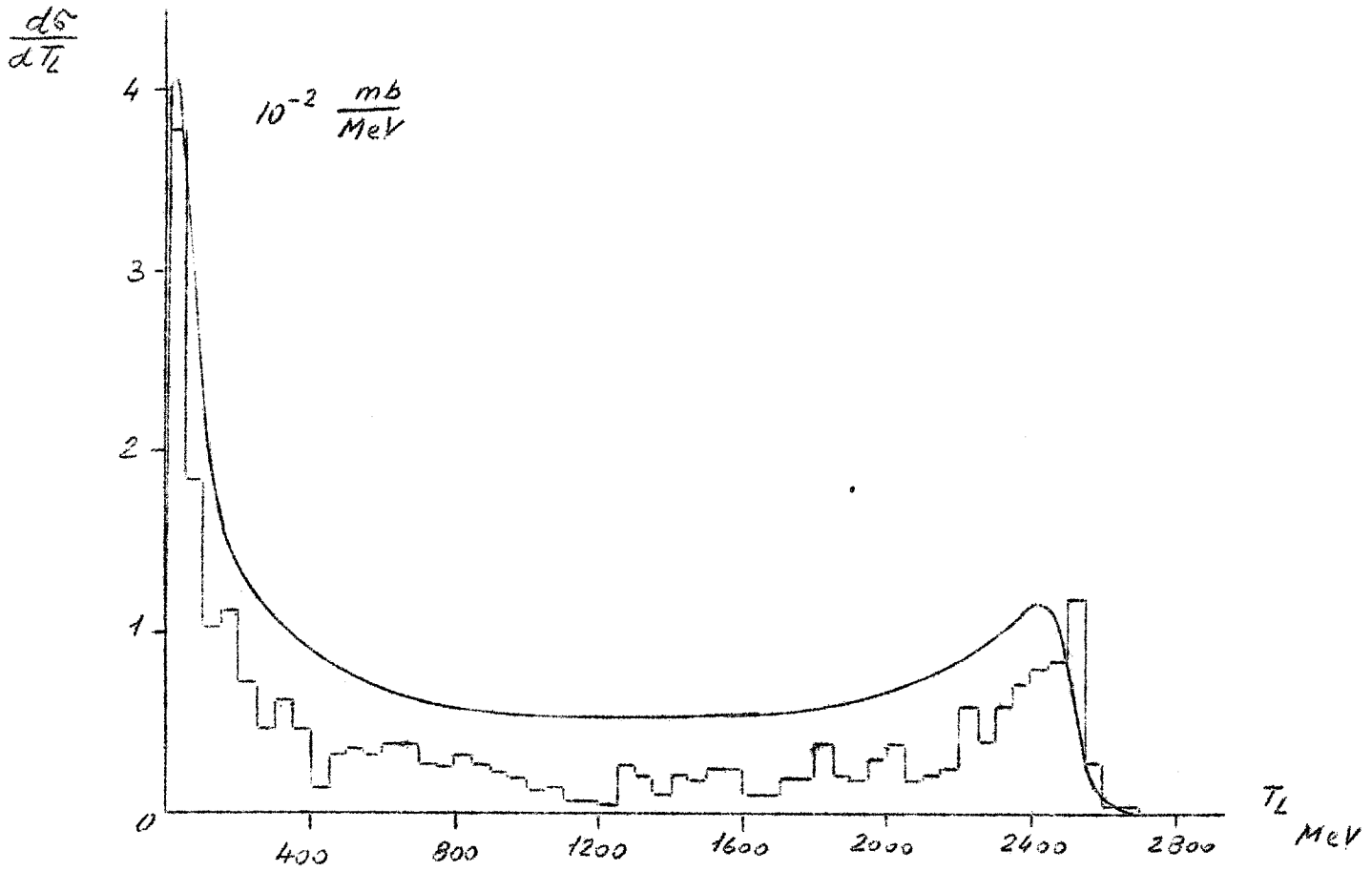

FIG. 3 – Theoretical and experimental spectrum of outgoing neutrons in the lab. system for the $p + p \rightarrow p + u + \pi^+$ reaction at 2.85 GeV of kinetic energy in lab. system of incoming protons.

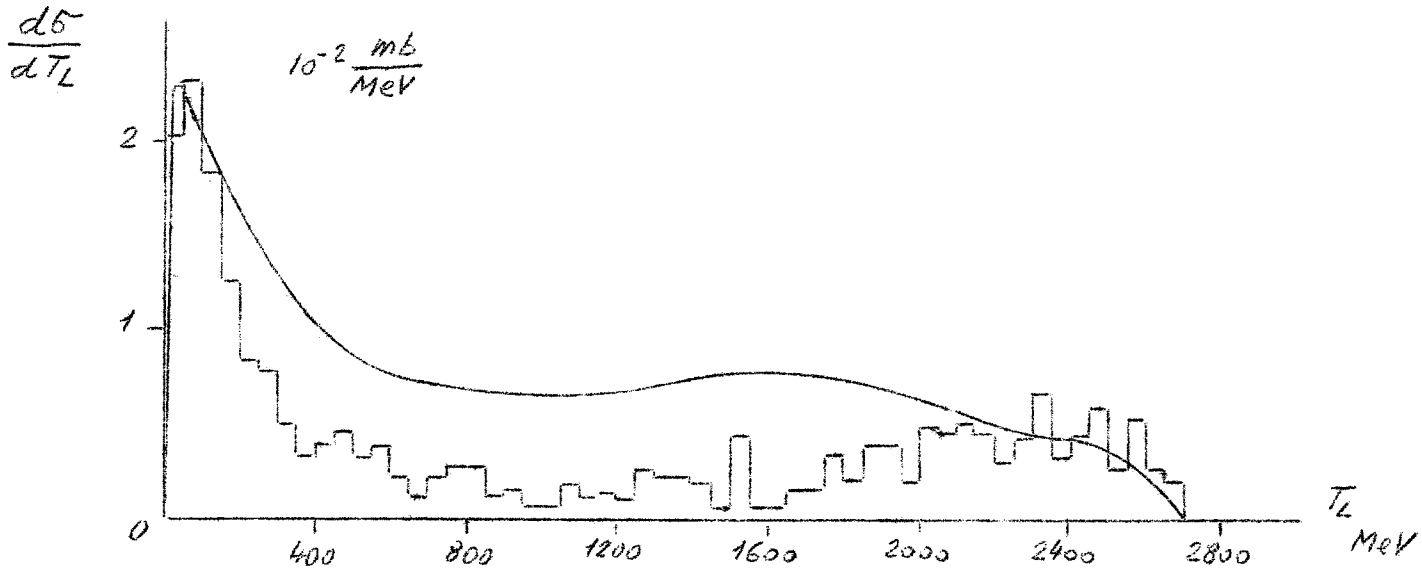

FIG. 4 - Theoretical and experimental spectrum of outgoing protons in the lab. system for the reaction $p + p \rightarrow p+u+ \pi^+$ at 2.85 GeV of kinetic energy in lab. system of incoming protons.

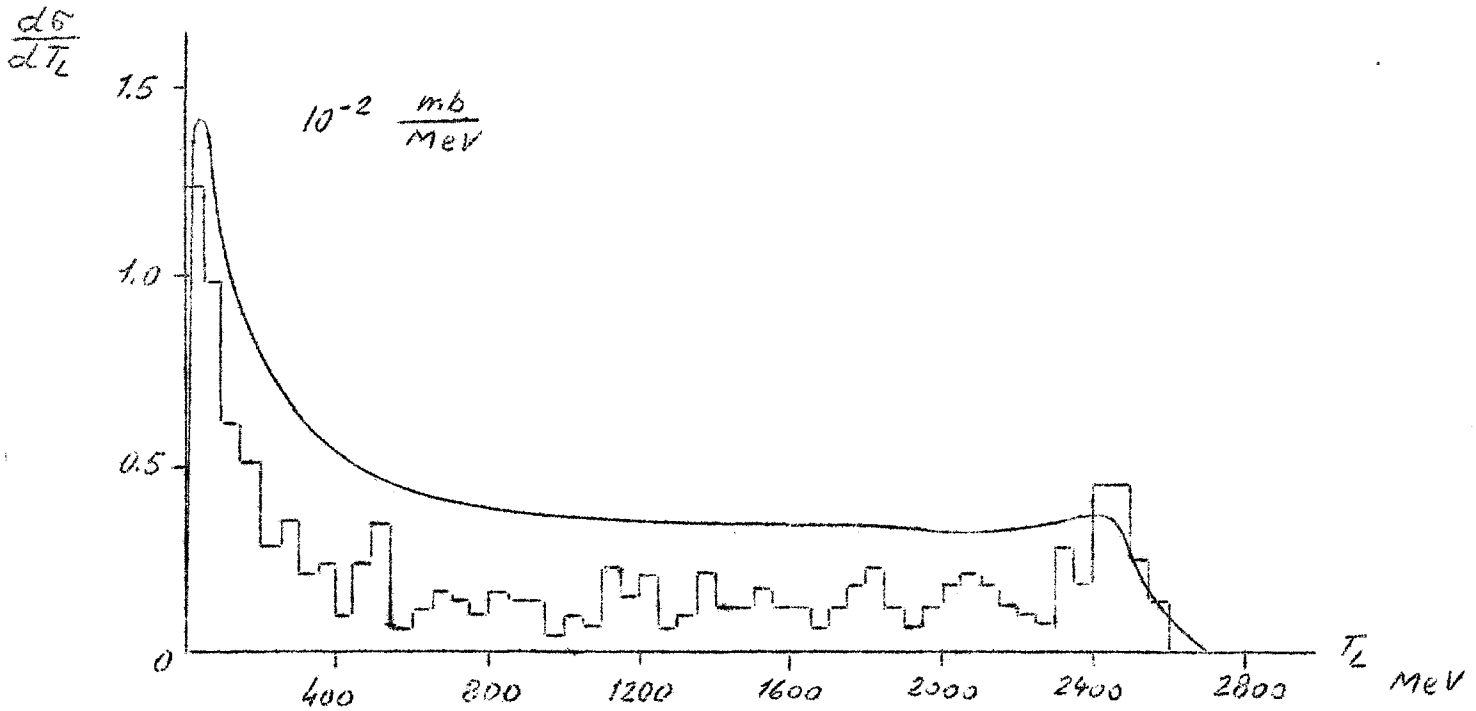

FIG. 5 - Theoretical and experimental spectrum of outgoing protons in the lab. system for the reaction p+p — p+p+π° at 2.85 GeV of kinetic energy in lab. system of incoming protons.